Journal of Structural Geology 32 (2010) 832–842

Contents lists available at ScienceDirect

Journal of Structural Geology

journal homepage: www.elsevier.com/locate/jsg

Control of shear zone location and thickness by initial grain size variations in upper mantle peridotites

Julie Newman [a,*], Martyn R. Drury [b]

[a] Department of Geology and Geophysics, Texas A&M University, College Station, TX 77843, USA
[b] Department of Earth Sciences, Faculty of Geoscience, Utrecht University, 3508TA Utrecht, Netherlands

ARTICLE INFO

Article history:
Received 22 February 2010
Accepted 2 June 2010
Available online 10 June 2010

Keywords:
Localization
Peridotite
Mylonite
Reaction
Grain size

ABSTRACT

The Turon de Técouère peridotite, North Pyrenean fault zone, France, contains protomylonites grading to ultramylonites. Grain size reduction to 0.005–0.025 mm took place by reaction during deformation. Within the protomylonite domain, the size of the porphyroclasts suggests an initial grain size in this domain of 2–10 mm. In the ultramylonite domain, porphyroclasts are polycrystalline with an internal grain size of 0.1–0.2 mm, indicating that the ultramylonite domain had a finer initial grain size than the protomylonite domain. Lattice-preferred orientations and misorientations within a polycrystalline porphyroclast in the ultramylonite domain suggest an early episode of dislocation creep accommodated dynamic recrystallization, restricted predominantly to the present-day ultramylonite domain. Later grain size reduction by reaction, resulting in very fine-grained ultramylonites, was concentrated in the same domain. For reaction-involved deformation, initial grain size may be crucially important as it controls the surface area available for nucleation of new grains. As a result of the finer initial grain size within the present-day ultramylonites, a critical percentage of fine-grained matrix developed in the present-day ultramylonite domain earlier than in the present-day protomylonite domain, resulting in localization of further deformation in the ultramylonites. This study suggests that zones of locally smaller grain size can act as heterogeneities that control the location and width of shear zones formed by reaction-softening.

1. Introduction

Strain localization has been widely researched and well documented in upper and middle crustal settings. While strain within the lower crust and upper mantle (within the "ductile regime") is often assumed to be homogeneous, field studies have documented localized deformation that took place in these rocks under the high pressures and temperatures prevalent in these settings (e.g., Boullier and Gueguen, 1975; Rubie, 1983; Nicolas, 1986; Rutter and Brodie, 1988; Handy, 1989; Drury et al., 1991; Vissers et al., 1991; Jaroslow et al., 1996; Denghui et al., 1998; Jin et al., 1998; Newman et al., 1999; Dijkstra et al., 2002; Michibayashi and Mainprice, 2004; Warren and Hirth, 2006; Warren et al., 2008; Webber et al., 2008, 2010; Toy et al., 2010). The processes responsible for strain localization in ductiley deforming rocks have been studied through field research, as well as experimental and theoretical investigations. Field studies have identified a number of mechanisms responsible for, or associated with, localization in ductiley deforming rocks, including grain size reduction by either dynamic recrystallization (Rutter and Brodie, 1988; Warren and Hirth, 2006) or by reaction (Brodie and Rutter, 1987; Handy, 1989; Furusho and Kanagawa, 1999; Kruse and Stünitz, 1999; Newman et al., 1999; Handy and Stünitz, 2002; Dijkstra et al., 2002), by the introduction of fluids (Brodie, 1980; Vissers et al., 1995) or melt (Dijkstra et al., 2002), or as a result of compositional variations (Toy et al., 2010; Webber et al., 2010). Experimental and theoretical investigations have extended our understanding of localization processes in ductiley deforming materials through quantitative evaluation of the influence of variables such as relative viscosities in polyphase materials, relative abundance and spatial distribution of "hard" and "soft" phases, and changing rheologies during deformation (e.g., Tharp, 1983; Jordan, 1987; Rutter and Brodie, 1988; Handy, 1994; Bloomfield and Covey-Crump, 1993; Govers and Wortel, 1995; Dell'Angelo and Tullis, 1996; de Bresser et al., 1998, 2001; Montési and Zuber, 2002; Holyoke and Tullis, 2006; Takeda and Griera, 2006; Jessell et al., 2009).

While the mechanisms responsible for localization have been explored, less attention has been devoted to the controls on the location and scale of localization in ductiley deforming rocks. Field, experimental and theoretical studies indicate that the initiation of

* Corresponding author.
E-mail address: newman@geo.tamu.edu (J. Newman).

0191-8141/$ – see front matter © 2010 Elsevier Ltd. All rights reserved.
doi:10.1016/j.jsg.2010.06.001

localized deformation requires a geometric heterogeneity. Within the upper and middle crust, fractures may provide sufficient heterogeneity to result in localized deformation, often aided by the introduction of fluids (e.g., Mitra, 1978; Beach, 1980; O'Hara, 1988, 1990; Fitz Gerald and Stünitz, 1993; Newman and Mitra, 1993; Stünitz and Fitz Gerald, 1993). Within the lower crust, where high temperatures and pressures do not favor fracturing, heterogeneities may be provided by variations in rock type or by zones through which fluids have been introduced. However, the upper mantle is thought to be compositionally more homogeneous than the crust, and free fluids may not always be present in the upper mantle (e.g., Newman et al., 1999).

We have attempted to determine the controls on location and scale of localization in mantle rocks, with respect to a shear zone developed within upper mantle peridotites and exposed as the Turon de Técouère peridotite body, France. Strain localization resulted, in part, from a reaction associated with decreasing temperatures and pressures. The deformation microstructures, deformation mechanisms and chemistry of these rocks are discussed in detail in Vissers et al. (1997) and Newman et al. (1999), and are reviewed below. This contribution focuses on polycrystalline porphyroclasts, observed only within the highest strain zone of the peridotite body that, when compared with less deformed rocks outside the high strain zone, suggest that a variation in grain size existed within these rocks prior to the reaction-enhanced deformation. For reaction-involved deformation, initial grain size is crucially important as it controls both the surface area available for nucleation of new grains and the length scale for diffusive mass transfer. We argue that the initial variation in grain size across the Turon de Técouère peridotite body that existed prior to the reaction-enhanced deformation served as the heterogeneity that determined the location and thickness of the high strain zone.

2. Background

Turon de Técouère is exposed in the Northern Pyrenean Zone, north of the North Pyrenean Fault. Alpine thrusting and subsequent erosion has brought the Variscan basement of the Axial Zone and the North Pyrenean peridotite massifs to the surface (Fig. 1a; Fabriès et al., 1991; Vissers et al., 1997). The Turon de Técouère peridotite is about 600 m across (Fig. 1b). The rocks exposed in the body are spinel- and plagioclase- bearing lherzolite mylonites. Protomylonites ($\sim$40% matrix) dominate the southwest portion of the body, with mylonites ($\sim$80% matrix) making up the northeast portion. A layer, about 25–40 m thick, of ultramylonites ($\sim$90% matrix) transects the mylonite domain at a low angle.

The mylonites at Turon de Técouère formed by a reaction-dominated deformation event (Newman et al., 1999). The fine-grained matrix was produced by neocrystallization as a result of a continuous net–transfer reaction written as:

$$\begin{aligned} &\text{orthopyroxene}_1 + \text{clinopyroxene}_1 + \text{spinel}_1 + \text{plagioclase}_1 \\ &+ \text{olivine}_1 = \text{orthopyroxene}_2 + \text{clinopyroxene}_2 + \text{spinel}_2 \\ &+ \text{plagioclase}_2 + \text{olivine}_2 \qquad (1) \end{aligned}$$

Changes in mineral chemistry, from porphyroclast compositions to matrix compositions, are consistent with this reaction occurring while temperatures were decreasing. Orthopyroxene in the matrix is depleted in Al and Ca relative to the porphyroclasts, clinopyroxene matrix grains are depleted in Na and Al relative to clinopyroxene porphyroclasts, and spinel matrix grains are depleted in Al and Mg. Olivine does not show large variations in compositions, but matrix grains contain higher Mg than porphyroclasts. Geochemical analyses of these phases are provided in Newman et al. (1999; Fig. 11 and Tables 1–3). This continuous reaction is associated with the transition from the medium-pressure spinel lherzolite metamorphic facies to the low-pressure plagioclase lherzolite facies at pressures around 0.5–1 GPa. Note that while plagioclase was not present in the initial spinel lherzolite assemblage, we have included plagioclase$_1$ as a reactant, because the chemical analyses of plagioclase grains suggest that they continued to react after formation (Newman et al., 1999). Geothermometry based on compositions of matrix grains formed during the reaction yield temperatures between 850 and 700 °C, while porphyroclasts yield higher temperatures ($\sim$1000 °C) (Newman et al., 1999).

Porphyroclasts in the protomylonites are approximately 0.2–1 cm in diameter, and the reaction resulted in the formation of fine new grains, 2–25 μm in diameter, observed within protomylonites, mylonites and ultramylonites. The fine-grained matrix within the mylonites and ultramylonites exhibits a weak lattice preferred orientation with a concentration of [100] perpendicular to the lineation (Newman et al., 1999, see Fig. 8b), few dislocations, and alignment of grain boundaries (Newman et al., 1999). These observations are consistent with deformation by grain-size sensitive creep (e.g., Boullier and Gueguen, 1975; Schmid et al., 1977; Brodie and Rutter, 1987; Drury and Humphreys, 1988; Passchier and Trouw, 2005; Sundberg and Cooper, 2008). Recent experimental results by Sundberg and Cooper (2008) particularly support this interpretation. They deformed fine-grained ($\sim$2–5 μm) olivine-orthopyroxene aggregates at low stresses ($<$20 MPa) and observed an olivine LPO similar to the one observed from the Turon de Técouère rocks, with olivine [100] perpendicular to the lineation. Sundberg and Cooper (2008) suggest that their samples deformed by diffusion-accommodated grain boundary sliding.

Weakening of the rocks, and strain localization, within the mylonite and ultramylonite domains resulted from a change in the dominant deformation mechanism from dislocation creep within porphyroclasts to diffusion creep within the fine-grained matrix.

3. High strain zone (present-day mylonite and ultramylonite domains)

Evidence for strain localization can be very difficult to ascertain within high-grade rocks. At Turon de Técouère, in addition to the increase in the percentage of fine-grained matrix from protomylonites to the ultramylonites, higher strains within the ultramylonites are suggested by variations in the thicknesses of the spinel-bearing pyroxenite layers within the protomylonite and mylonite domains. Within the protomylonite domain, the pyroxenite layers are typically between 2 and 5 cm thick (Fig. 2a). Pyroxenite layers within the mylonite domain are generally only 1–2 cm thick (Fig. 2b), and are often cross-cut by local bands, $<$1 cm thick, of ultramylonites (zones that contain a slightly higher percentage of matrix ($>$90%)). Within the ultramylonite domain, pyroxenite layers are rarely observed. The progressively decreasing thickness of the pyroxenite bands suggests a progressive increase in strain, and thinning out of the bands, from the protomylonites to the mylonites to the ultramylonites.

In addition, the ultramylonites transect the mylonite domain at a low angle, suggesting that at least some deformation within the ultramylonite domain occurred later than within the mylonites, and accommodated additional strain. This is further supported by the thin ultramylonite zones that transect, and cross-cut, pyroxenite layers within the mylonite domain.

While the percentage of matrix grains is very similar between the mylonites and ultramylonites (80% vs. 90%), there exist other aspects of their microstructures that suggest that the ultramylonites may

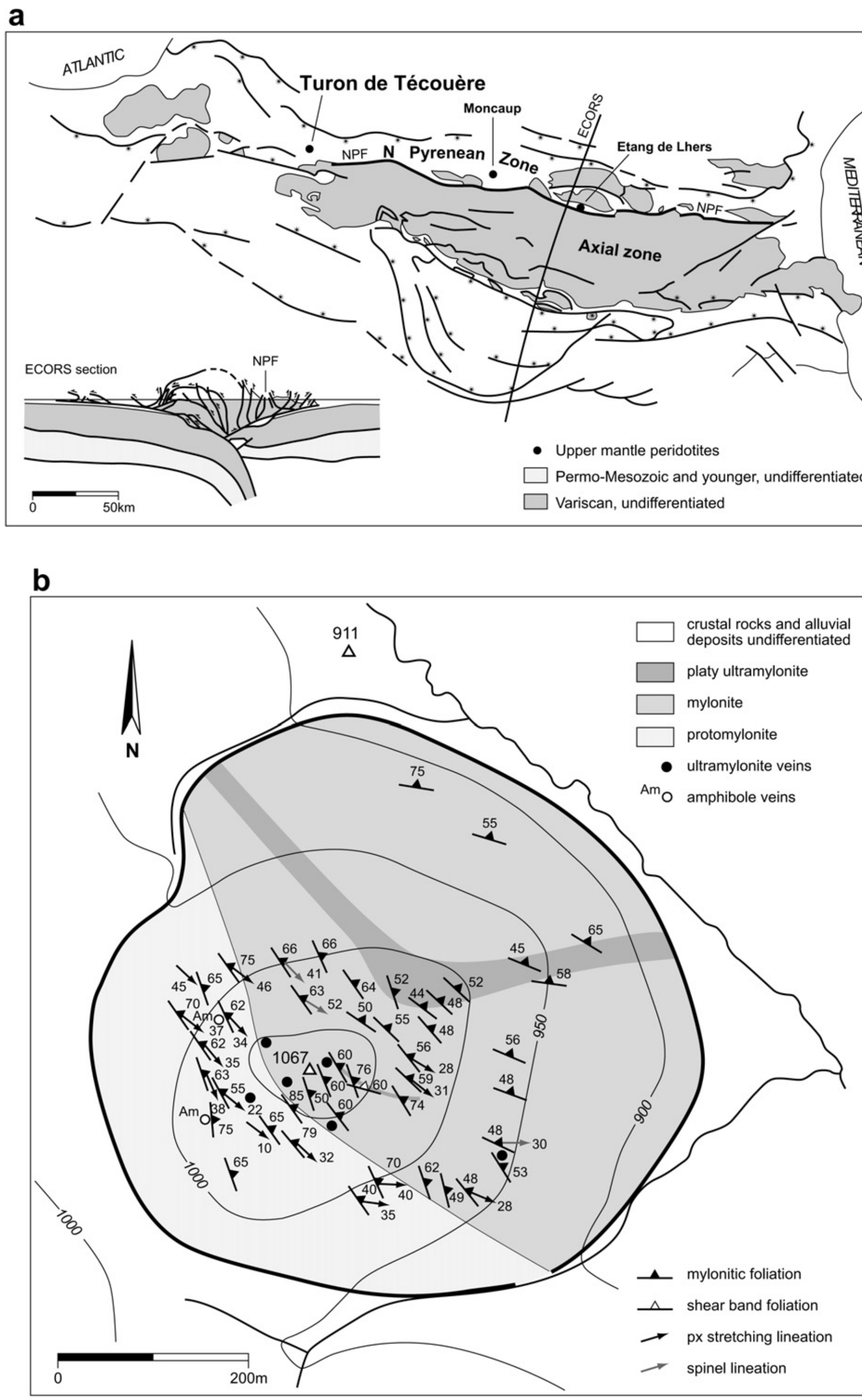

Fig. 1. (a) Structural sketch map of the Pyrenees, showing the location of the Turon de Técouère and other peridotite bodies. Cross-section based upon ECORS deep seismic reflection study (ECORS, 1988). NPF – North Pyrenean Fault. (b) Structural map of Turon de Técouère showing distribution of main mylonitic domains.

have accommodated greater strain. First, there exists a compositional layering in these rocks of olivine-orthopyroxene bands alternating with more polyphase bands (olivine, plagioclase and Cr-spinel); this layering is better developed within the ultramylonites than in the mylonites. The polyphase bands are generally finer-grained (2–10 μm) than the olivine-orthopyroxene bands (5–25 μm) and are more continuous and better defined within the ultramylonites (compare Fig. 2c and d). In the ultramylonites, the foliation is defined by a dimensional preferred orientation of the grains, parallel to the foliation, as well. For example, the longest grain diameters of olivine and orthopyroxene grains tend to be parallel to the foliation within the ultramylonites, while in the mylonites there is significant variation in the angles between the longest grain diameters and the foliation (Fig. 3). In addition, grain boundary alignments, suggesting deformation by grain boundary sliding, are best developed in the ultramylonite domain (Fig. 2e). While we cannot quantitatively determine the contribution of grain boundary sliding to the strain in these rocks, the well-developed alignments in the ultramylonites suggest that they may have accommodated greater strains within the ultramylonites than in the mylonites.

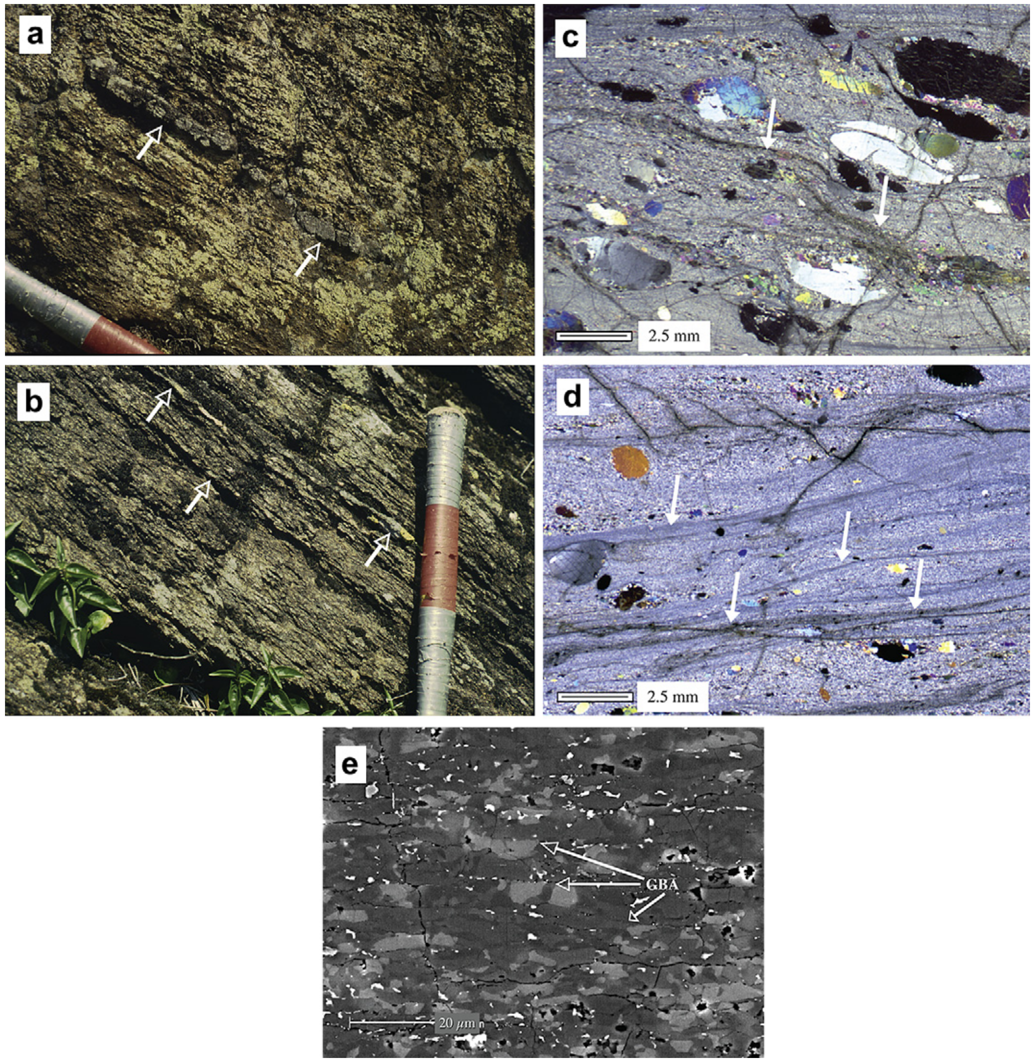

Fig. 2. (a) Pyroxenite band (arrows) in protomylonite. Band is ~3 cm thick (width of hammer handle 4 cm) (b) Pyroxenite bands (arrows) in mylonite. Bands are ~1 cm thick. (c and d) Foliation in mylonite (c) and ultramylonite (d) samples. Light colored bands are composed of predominantly olivine and orthopyroxene. Thin dark-colored bands are more polyphase composed of spinel, clinopyroxene and plagioclase, in addition to olivine and orthopyroxene. Compositional banding is more continuous in ultramylonite samples. Cross-polarized light. (e) Grain boundary alignments (indicated by arrows) in a polyphase band. Ultramylonite. Backscattered electrons (BSE). Decorated thin section (Kohlstedt et al., 1976).

The geometry of porphyroclast systems can also provide estimates of the minimum amount of local shear strain. For delta and sigma clasts, the total length of the matrix tails or wings derived from the porphyroclast divided by the diameter of the clast gives the minimum local shear strain accumulated in the vicinity of the porphyroclast (Van den Driessche and Brun, 1987; ten Brink, 1996). Based on spinel delta and sigma clasts, local shear strain estimates of 6–25 are obtained for the ultramylonites and local shear strains < 5 for the mylonites.

4. Polycrystalline porphyroclasts

Polycrystalline porphyroclasts, lozenge shaped porphyroclasts, 0.1 cm–0.5 cm in diameter, composed of intermediate-size (50–200 μm) olivine grains or pyroxene grains are observed within the ultramylonite zone, and, rarely, within the mylonite domain close to the ultramylonite domain (Fig. 4a). The long axes of these lozenge shaped clasts are parallel to the mylonitic foliation. They have not been observed within the protomylonite domain. Porphyroclasts within the protomylonite domain are single crystals and vary in size from approximately 0.2–1 cm. Geochemical analyses of the intermediate-size grains within the polycrystalline porphyroclasts indicate compositions similar to the porphyroclasts (Newman et al., 1999).

The intermediate-size grains that make up the polycrystalline porphyroclasts show polygonal grain shapes. Straight grain boundaries and triple junctions are common (Fig. 4). Occasionally, the intermediate-size pyroxene or olivine grains mantle clinopyroxene or olivine porphyroclasts, respectively (Fig. 4b). The central clasts typically show substructure (Fig. 4c, e, and Fig. 5a), also observed in some of the intermediate-size grains (Fig. 5b). Insertion of the gypsum plate when viewing the polycrystalline porphyroclasts in crossed-polarized light suggests that the intermediate-sized grains and the central clasts have similar lattice preferred orientations (Fig. 4d). The olivine-rich polycrystalline porphyroclasts frequently contain some orthopyroxene and spinel grains of approximately the same grain size as the olivine (Fig. 6). Fine-grained reaction products are observed around the outside of the polycrystalline porphyroclasts, but also frequently along grain boundaries within many polycrystalline porphyroclasts (Fig. 4).

Investigation of olivine polycrystalline porphyroclasts using decorated samples (e.g., Kohlstedt et al., 1976) on the scanning electron microscope reveals that most olivine grains in the

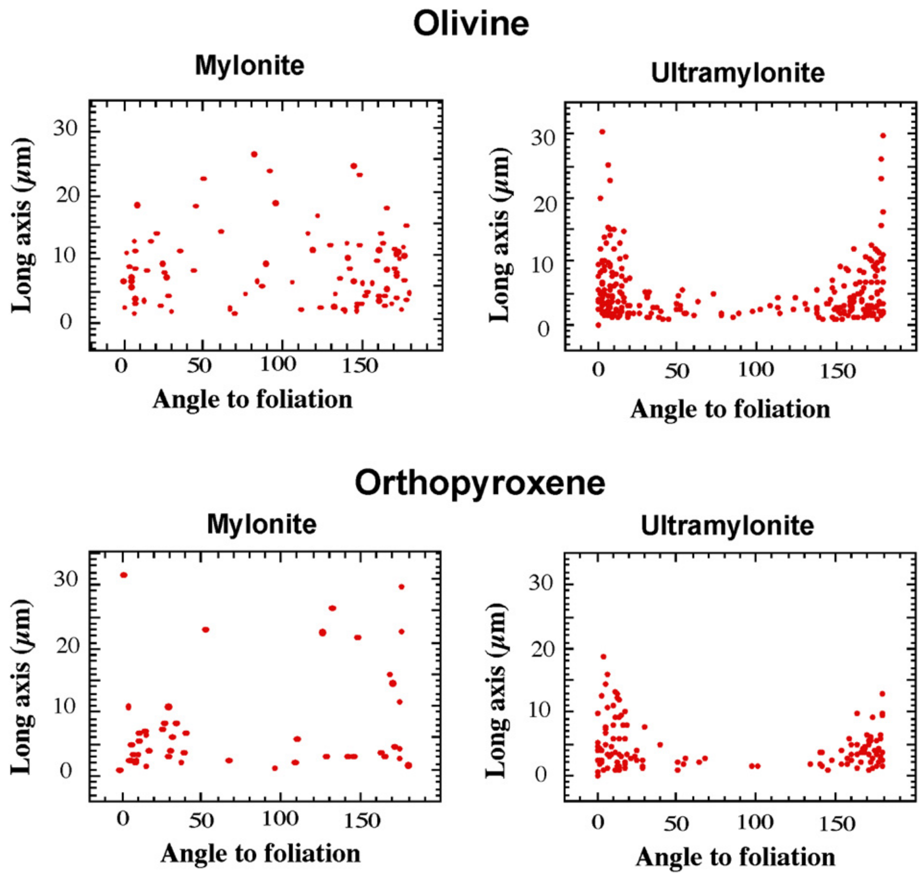

Fig. 3. Length of long axes of olivine and orthopyroxene grains vs. the angle of the axes to the foliation.

polycrystalline porphyroclasts contain substructure (Fig. 5). Subgrain boundaries are straight and tend to be similarly spaced as in porphyroclasts within the ultramylonite and mylonite domains (mean subgrain size 8.7 μm and 9.5 μm, respectively). All porphyroclasts, including the polycrystalline porphyroclasts, contain higher dislocation densities than matrix grains, and porphyroclasts in protomylonites contain higher dislocation densities ($1.17 \times 10^{13}/m^2$) than porphyroclasts in mylonites ($2.85 \times 10^{12}/m^2$) and ultramylonites ($3.35 \times 10^{12}/m^2$).

4.1. Lattice preferred orientation and misorientation in a polycrystalline porphyroclast

The microstructure and lattice preferred orientations in one polycrystalline porphyroclast from an ultramylonite have been studied using electron backscattered patterns on a scanning electron microscope (e.g., Prior et al., 1999). The polycrystalline porphyroclast is composed predominantly of olivine, with minor orthopyroxene and spinel (Fig. 6). Individual grains in the polycrystalline porphyroclast range from 25 to 150 μm in diameter. In the center of the polycrystalline porphyroclast is a larger olivine grain (400 μm diameter) that is likely a remnant of a former porphyroclast.

The grains that make up the polycrystalline porphyroclast show a preferred orientation with [100] forming a broad point maximum at a low angle (~15°) to the lineation within the ultramylonites, and [010] forming a broad point maximum subperpendicular to the foliation and lineation within the ultramylonites (Fig. 7a).

The large olivine grain in the center of the polycrystalline porphyroclast contains many subgrains that accommodate a cumulative lattice misorientation of 15° across the grain (Fig. 7b). The general orientations of these subgrains are close to the point maximum defined by the grains surrounding the central grain. Most of these subgrain boundaries are very low angle subgrains with misorientations less than two degrees, but several boundaries occur with higher misorientations ranging between 2 and 7° (Fig. 6). Polygonal, intermediate-sized grains are separated from the large central grain by intermediate angle boundaries with misorientations ranging from 15 to 50° (Fig. 6). Subgrains within the polygonal grains show similar spacings as within the central clast (compare Fig. 5a and b).

Misorientation angles across olivine grain boundaries have been measured throughout the polycrystalline porphyroclast. The misorientation angle distribution (MAD) shows a roughly bimodal distribution, with most boundaries either low angle boundaries ($\varphi < 5°$) or high angle boundaries ($\varphi = 75–110°$) (Fig. 8a). The MAD of low angle subgrain boundaries is strongly skewed towards low angles (Fig. 8b). Most low angle boundaries have misorientations less than 2°, but there is a significant number of higher angle subgrain boundaries ($\varphi = 2–12°$). Fig. 8c shows a plot of cumulative lattice misorientation across the large central grain and the adjacent polygonal grains. The misorientation across individual boundaries and the cumulative misorientation across the grain both tend to increase away from the center of the large grain. Several of the polygonal grains have similar orientations to the adjacent part of the large grain (Fig. 8c).

5. Discussion

5.1. Development of polycrystalline porphyroclasts

The microstructures of the polycrystalline porphyroclasts suggest that the intermediate-size (50–200 μm) polygonal grains that compose these clasts, and the intermediate-sized grains

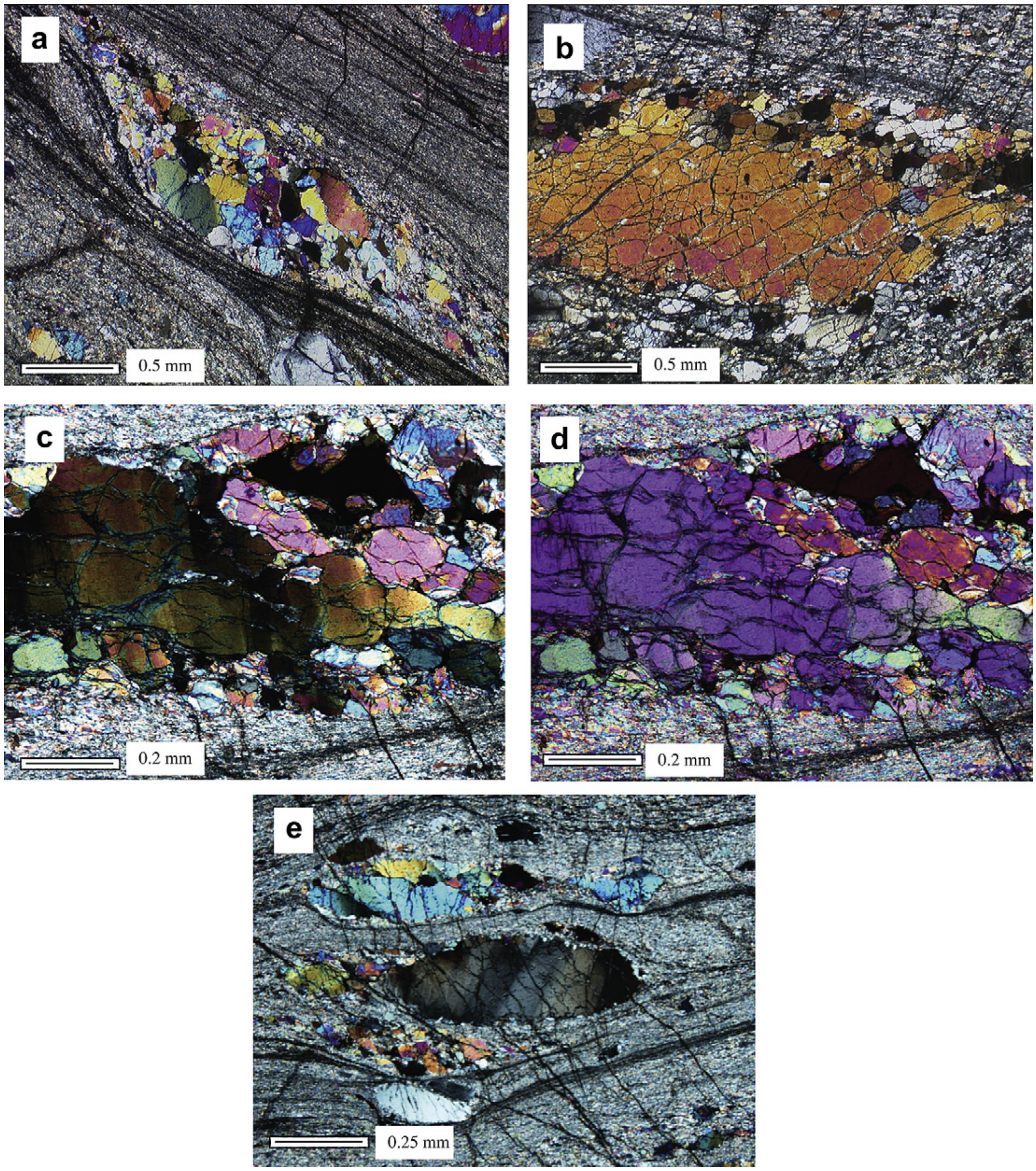

Fig. 4. Optical photomicrographs, crossed-polars. (a) Polycrystalline porphyroclast within an ultramylonite. Clast is composed of olivine grains, with minor orthopyroxene. (b) Intermediate-size (50–200 μm) grains mantle a large olivine clast within an ultramylonite. (c) Olivine clast with subgrains mantled by intermediate-size grains. (d) Image of same area as shown in c, with gypsum plate inserted. Intermediate-size grains have similar orientation as central clast. (e) Olivine clast showing subgrain development.

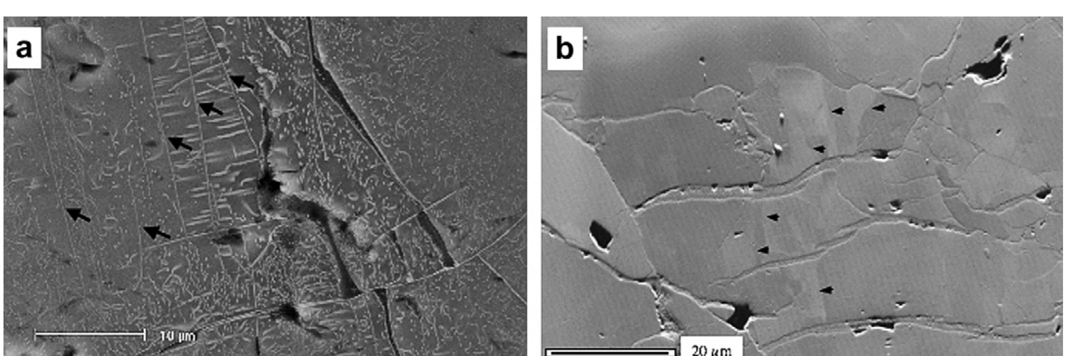

Fig. 5. (a) Subgrains (arrows) within the large central clast of a polycrystalline porphyroclast within an ultramylonite. Other white lines and points are dislocations. Decorated thin section imaged with BSE. (b) Subgrains (arrows) within intermediate-size grains of a polycrystalline porphyroclast. Ultramylonite. Orientation contrast imaging (forescattered BSE) on SEM.

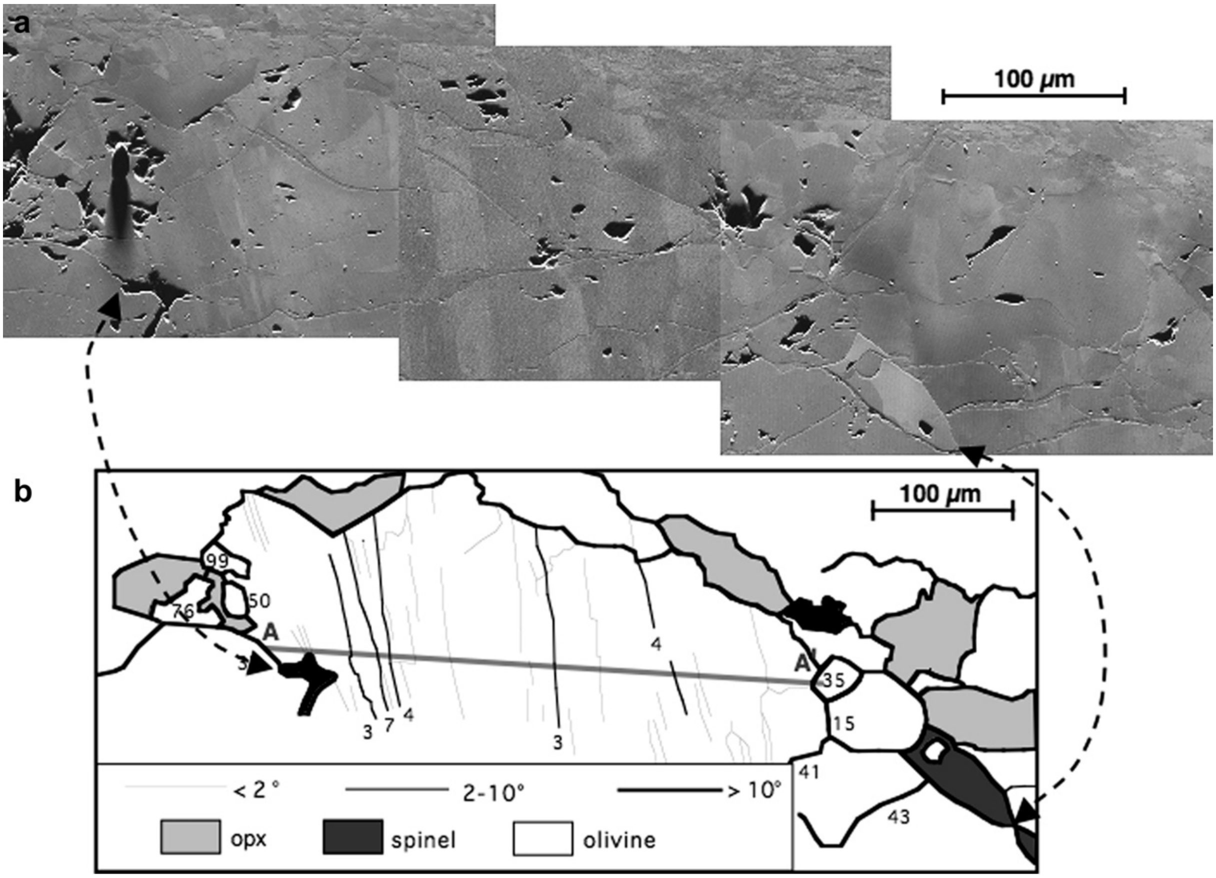

Fig. 6. (a) Orientation contrast images (forescattered BSE) across portion of polycrystalline porphyroclast. Ultramylonite sample. (b) Sketch of boundary misorientations in (a). Gray line (A–A′) indicates transect across boundaries shown graphically in Fig. 7c. Numbers indicate misorientation angle, in degrees, of adjacent boundary. Large central clast is enclosed by grain boundaries with >10° misorientation.

(50–200 μm) observed at the margins of some porphyroclasts, have formed by dislocation creep accommodated dynamic recrystallization. The [100] of grains that make up the polycrystalline porphyroclast studied in detail cluster at a small angle to the lineation and [010] are subperpendicular to the foliation, consistent with high temperature dislocation creep ([100](010)-slip) in olivine (Nicolas and Poirier, 1976). Also, the misorientation angle distribution is typical for materials that have deformed by dislocation creep with concurrent recovery and recrystallization involving the development of new high angle grain boundaries by subgrain rotation (Trimby et al., 1998, 2000; Fliervoet et al., 1999). The key feature of the MAD is the occurrence of high angle subgrains and new high angle grain boundaries. If recrystallization occurs by extensive grain boundary migration, individual grains are swept by grain boundaries before significant subgrain misorientations can develop (Trimby et al., 2000; Neumann, 2000). The polygonal grain shapes of the intermediate-sized grains and irregular shape of the grain boundaries of the porphyroclasts they mantle suggest that grain boundary migration may also have contributed to the formation of the recrystallized grains. These findings suggest that dislocation creep accommodated dynamic recrystallization was the dominant deformation mechanism in the polycrystalline porphyroclasts. The LPO's are consistent with dynamic recrystallization at temperatures greater than 950 ± 50 °C (Nicolas and Poirier, 1976), which is in agreement with geothermometry on polycrystalline porphyroclasts reported by Newman et al. (1999) suggesting that the dynamic recrystallization occurred at ~1000 °C. The changes in the mineral chemistry between the polycrystalline porphyroclasts and the fine grains in the matrix suggest that the deformation dominated by dynamic recrystallization occurred earlier, at higher temperatures, than the deformation dominated by reaction and grain-size sensitive creep. In addition, we note that many of the intermediate-size grains contain very fine grains (2–25 μm) along their grain boundaries (Fig. 4), suggesting the reaction-dominated event overprinted the earlier deformation.

Two factors suggest that some static recrystallization occurred following the dislocation creep and concurrent recrystallization, but prior to the reaction-dominated deformation event. First, the relatively straight grain boundaries of the intermediate-size grains within the polycrystalline porphyroclasts are consistent with a reduction in the grain boundary lobateness typically associated with dynamic recrystallization (Heilbronner and Tullis, 2002). Second, the distinctly polygonal shapes of the intermediate-size grains resemble the foam geometry expected for static recrystallization (e.g., Heilbronner and Tullis, 2002).

The dynamic recrystallization dominated deformation and the reaction-dominated deformation may, therefore, be considered separate events, possibly separated by some static recrystallization. The closely spaced very low angle subgrain boundaries observed in the large central grain and in the smaller polygonal grains were probably produced during the later lower temperature reaction-dominated deformation event.

5.2. Controls on scale and location of shear zone

Strain localization along the Turon de Técouère shear zone occurred as a result of grain size reduction by reaction. Evidence for the reaction is observed in all of the mylonite domains at Turon de

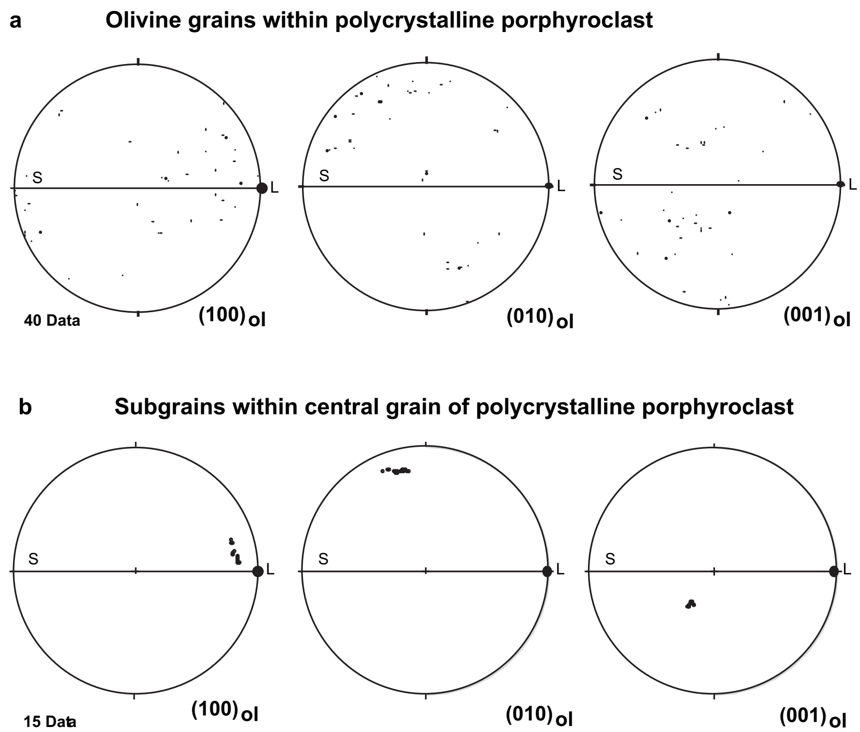

Fig. 7. (a) Lattice preferred orientations (LPO) of olivine grains within a polycrystalline porphyroclast within an ultramylonite sample. [100] axes show point maximum close to the lineation and [010] perpendicular to the foliation and lineation suggesting deformation by a-slip. (b). LPO of subgrains within the large central grain of a polycrystalline porphyroclast. S = foliation plane, L = lineation.

Técouère, but the highest proportion of fine-grained matrix (2–25 μm) produced by reaction, and the highest strain, is concentrated in the present-day mylonite and ultramylonite domains. We suggest that the reaction was localized into these zones because of the pre-existing finer grain size (50–200 μm).

The polycrystalline porphyroclasts, and the porphyroclasts surrounded by intermediate-size grains, formed by dislocation creep accommodated dynamic recrystallization at temperatures of ~1000 °C, and are observed only in the present-day ultramylonite and mylonite zones, suggesting that the high temperature deformation event was restricted to the area that now comprises these zones. No evidence for dynamic recrystallization is observed in the protomylonite domain. The high temperature deformation was followed by a period of static recrystallization. Later deformation and grain size reduction by reaction (850–700 °C) resulted in the development of the present-day mylonites and ultramylonites in the same zone that experienced the earlier high temperature deformation. The later and lower temperature deformation took place by a different mechanism (reaction to a very fine grain size and grain size sensitive creep) than the earlier deformation (dislocation creep accommodated dynamic recrystallization).

The 50–200 μm grains that compose the polycrystalline porphyroclasts observed in the ultramylonite domain indicate the initial grain size (~50–200 μm) in the ultramylonite domain before the reaction and associated grain size reduction. The cm-scale porphyroclasts in the protomylonite domain indicate the initial grain size (cm-scale) in the protomylonite domain. Therefore, grain size varied across the region prior to the beginning of the deformation event dominated by reaction.

Grain boundaries and dislocations act as sites for easier nucleation, enabling nuclei to be formed with lower activation energies than in homogeneous crystals (e.g., Spry, 1983; Brodie, 1980 and others listed within), so that the nucleation rate may be increased. A similar effect of initial grain size on nucleation of dynamically recrystallized grains is known from cubic metals (Sakai and Jonas, 1984). Enhanced nucleation may also result from greater disequilibrium as a consequence of higher dislocation densities (e.g., Wintsch and Dunning, 1985; Stünitz, 1998). The porphyroclasts in the protomylonites in these rocks contain higher dislocation densities than porphyroclasts within the mylonites and ultramylonites. Disequilibrium resulting from higher dislocation densities, therefore, might be expected to result in higher rates of nucleation in the protomylonites than in the ultramylonites. As we see the opposite effect, greater nucleation of new phases in the present-day ultramylonite and mylonite domains than in the protomylonite domain, we suggest that the finer grain size in the present-day ultramylonite domain was dominantly responsible for enhanced nucleation. The finer grain size resulted in greater grain boundary surface area available to act as sites for nucleation of new grains. In addition the initial grain size controls the length scale of mass transfer needed for the local reactions along the grain boundaries. Therefore, the percentage of fine-grained (2–25 μm) matrix, produced by reaction, increased more rapidly in the finer-grained domain (the present-day ultramylonite domain) than in the coarser-grained domain (the present-day protomylonite domain).

In the Turon de Técouère rocks, the fine-grained (2–25 μm) matrix deformed by diffusion accommodated grain size sensitive creep and was therefore weaker than coarser grains (porphyroclasts and polycrystalline porphyroclasts) that deformed by dislocation creep. The fine-grained matrix, therefore, constituted the "weak" phase, while the porphyroclasts constituted the "strong" phase. Experimental and theoretical studies have investigated localization processes in 2-phase materials (see review by Jessell et al., 2009). Most of these studies have suggested that when a critical percentage of a weak phase has been created within a rock, the rheology of the rock as a whole will be controlled by the

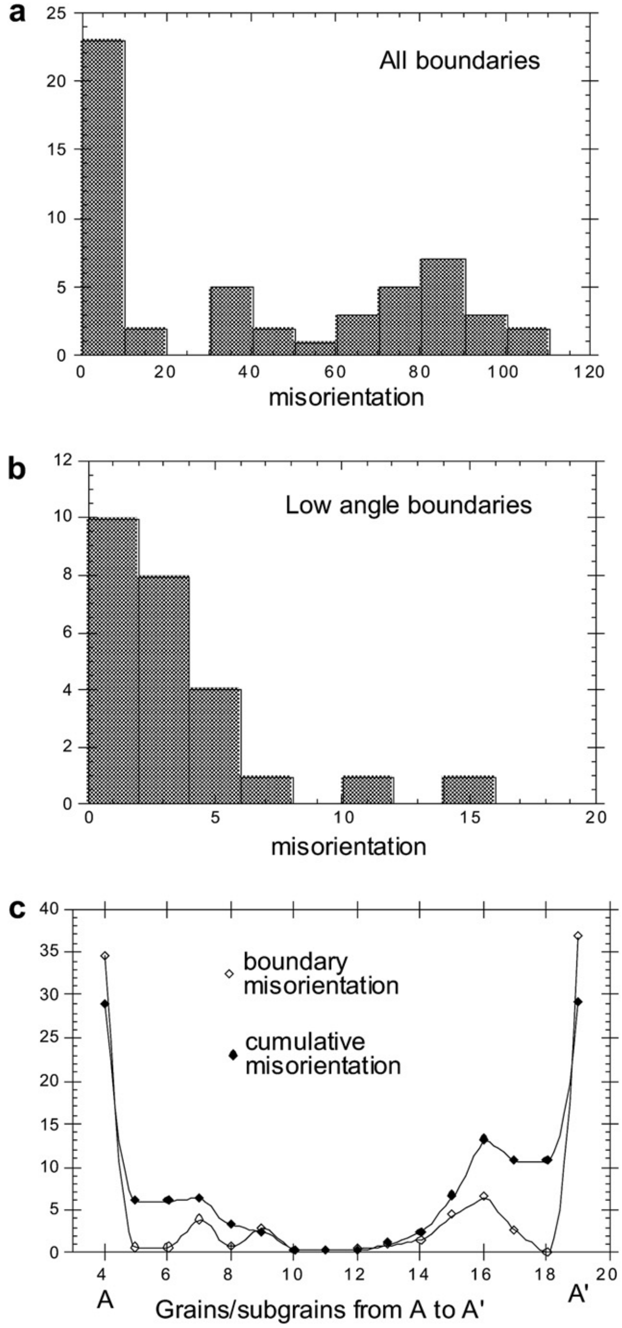

Fig. 8. Boundary misorientations within a polycrystalline porphyroclast. (a) Misorientation angles across boundaries of all adjacent olivine grains measured within a polycrystalline porphyroclast. (b) Low angle boundaries only (<20° misorientation). (c) Boundary misorientations (open circles) and cumulative misorientations (closed circles) in transect (A–A′) across large grain and some adjacent grains within the polycrystalline porphyroclast shown in Fig. 6.

strength of the weaker phase; most studies indicate that this transition will occur at 20–30% weak phase (e.g., Tharp, 1983; Rutter and Brodie, 1988; Jordan, 1987; Handy, 1994; Jessell et al., 2009 and references therein). Moreover, the contiguity of the weak phase may be more important that the absolute percentage of weak phase, with ~30% weak phase necessary for that phase to form a connected matrix or load-bearing network (e.g., Handy, 1990; Bloomfield and Covey-Crump, 1993; Dell'Angelo and Tullis, 1996; Takeda and Griera, 2006; Jessell et al., 2009).

Grain size reduction by dislocation creep accommodated dynamic recrystallization in the present-day mylonite and ultramylonite domains, during the earlier deformation event, resulted in a finer grain size (50–200 μm) in these domains, relative to the present-day protomylonite domain. The finer grain size resulted in greater surface area available for reaction during the reaction-dominated deformation event. Therefore, the percentage of fine-grained (2–25 μm) matrix increased to a critical percentage of the rock within the mylonite and ultramylonite domains, so that the strength of these rocks became matrix controlled while the strength of the rocks in the present-day protomylonite domain remained controlled by the porphyroclasts. Strain localization occurred because the contrast in stress or strain rate between the fine-grained (matrix-controlled) zone and the coarser-grained zone resulted in a sufficient heterogeneity between the two zones (e.g., White et al., 1980; Bloomfield and Covey-Crump, 1993; Govers and Wortel, 1995; Montési and Zuber, 2002; Jessell et al., 2009).

The localization in the present-day mylonite and ultramylonite domains may be considered a combination of "inherited" localization and "dynamic" localization, as defined by Montési and Zuber (2002). "Inherited" localization is controlled by pre-existing zones of weakness (e.g., compositional heterogeneities or zones along which alteration has taken place), while "dynamic" localization results from evolving microstructures during deformation. The pre-existing structure in the present-day mylonite and ultramylonite domains (50–200 μm grains) was not necessarily weaker than the cm-scale porphyroclasts in the protomylonite (during a deformation dominated by dislocation creep). However, the 50–200 μm grains in the present-day mylonite and ultramylonite domains evolved differently during deformation than the present-day protomylonite domain, nucleating a very fine-grained matrix, and achieving a "weak" phase controlled network (deforming by diffusion accommodated grain-size sensitive creep), while deformation in the protomylonite domain was controlled by dislocation creep in cm-scale porphyroclasts. The "zone of weakness" evolved during the deformation ("dynamic" localization) as a result of a pre-existing microstructural heterogeneity.

In the Turon de Técouère rocks, the source of the variation in grain size was a pre-existing shear zone. This leads to the question of what controlled the location of this earlier deformation. Unfortunately, there remains too little microstructural evidence and, in particular, too little spatial information from this early high temperature deformation event to answer this question.

5.3. Mylonite vs. ultramylonite domains

Both the mylonites and the ultramylonites show significantly higher percentage of fine-grained matrix (80% and 90%, respectively) than the protomylonites (40%). Both the mylonite and ultramylonite domains show evidence for the earlier higher temperature deformation event, although the polycrystalline porphyroclasts in the ultramylonite domain, when compared with the porphyroclasts rimmed with intermediate-size grains in the mylonite domain, suggest that the earlier deformation event was concentrated in the present-day ultramylonite domain.

While the mylonite and ultramylonite domains show similar microstructures, there is evidence, discussed above, suggesting that the ultramylonite rocks accommodated higher strain than the mylonites. While a critical percentage of fine-grained matrix, and contiguity of that matrix, is necessary for the rheology of the rock to be controlled by the matrix (e.g., Tharp, 1983; Jordan, 1987; Rutter and Brodie, 1988; Handy, 1990, 1994; Bloomfield and Covey-Crump, 1993; Takeda and Griera, 2006; Jessell et al., 2009), the variation in strain between the mylonite and the ultramylonite in these rocks suggests that other variables have influenced the strength of these rocks.

An increase in strain from the mylonites to the ultramylonites may be partly a result of the slightly higher percentage of fine-grained matrix. A critical volume fraction of matrix may be necessary for the destruction of the load supporting framework of large grains, but once this threshold has been passed, the strength may still depend on the volume fraction of matrix. This effect will be stronger within rocks that are deforming with a linear or near linear viscosity (i.e., diffusion accommodated grain-size sensitive creep, as inferred for these rocks) than in rocks deforming according to a non-linear flow law (e.g., Jessell et al., 2009).

The microstructures developed during deformation, however, may also exert a strong influence on the strength (e.g., Handy, 1990). We have observed several differences in microstructures between the mylonites and ultramylonites, including better developed compositional layering of olivine-orthopyroxene bands alternating with more polyphase bands (mainly olivine, plagioclase and Cr-spinel) within the ultramylonites (Fig. 2c and d). The polyphase bands are finer-grained (2–10 μm) than the olivine-orthopyroxene bands (5–25 μm). Deformation of the fine-grained matrix is inferred to have taken place by diffusion accommodated grain-size sensitive creep according to the general equation:

$$\dot{\varepsilon} = A\left(\frac{\sigma^1}{d^3}\right)e^{\left(\frac{-H}{RT}\right)} \quad (2)$$

where d = grain size, σ = stress, and $\dot{\varepsilon}$ = strain rate. As strain rate varies with grain size to d^3, the finer grain size in the polyphase bands, which are very well developed within the ultramylonites, may have resulted in lower stresses and faster strain rates, allowing the accommodation of higher strains. It is possible that olivine-plagioclase aggregates are also intrinsically weaker than olivine-orthopyroxene aggregates (Furusho and Kanagawa, 1999), although, experimental studies for grain-size sensitive creep in feldspar (Wang et al., 1996; Wang and Ji, 2000; Rybacki and Dresen, 2004) suggests that olivine and plagioclase have similar strength at the same grain size.

The presence of the polycrystalline porphyroclasts predominantly within the ultramylonite domain suggest that the intermediate-size grains (50–200 μm), formed by dynamic recrystallization at 1000 °C, were more prevalent within the present-day ultramylonite domain than in the present-day mylonite domain. Thus, the percentage of fine-grained matrix may have accumulated more rapidly within the present-day ultramylonite domain. As deformation progressed, the ultramylonite matrix may have had greater time and opportunity for the rearrangement of the microstructure into bands with different compositions and grain sizes, and forming grain boundary alignments, allowing for increased strains.

6. Conclusions

Strain localization occurred as a result of a change in the dominant deformation mechanism from dislocation creep in porphyroclasts to grain-size sensitive creep in the fine-grained matrix as the percentage of fine-grained matrix, produced by reaction, increased in these rocks. The percentage of fine-grained matrix increased more rapidly in the ultramylonite domain relative to the protomylonite domain because there was a pre-existing fine grain size in the present-day ultramylonite domain. The finer initial grain size provided greater grain boundary surface area for the nucleation of new grains and a reduced length scale for diffusive mass transfer, resulting in rapid grain size reduction in the ultramylonite domain. The more rapid grain size reduction within the ultramylonite domain, relative to the protomylonite and mylonite domains, led to localization of the strain in the present-day ultramylonite domain.

The variables that influence the scale and location of shear zones are complex, and may include: pre-existing structure or microstructure; prevailing pressure, temperature and fluid conditions as well as changes in these variables over time; and changes in microstructure and/or mineralogy that occur during deformation. Changes in microstructure during deformation, in particular, may result in single localized shear zones accommodating large displacements over time (e.g., Schmid et al., 1977; Mitra, 1984; Handy, 1989).

In the Turon de Técouère rocks, strain localization resulted from the combination of an inherited microstructural variation across the zone (i.e., grain size variation) and a change in microstructure induced during shearing (grain size reduction by syntectonic reaction). The response of the inherited microstructure to deformation during changing pressure and temperature conditions over time controlled the scale and location of the reaction-enhanced shear zone.

Acknowledgments

The electron microscopy studies reported in this paper were conducted at EMU, the Utrecht University Center for Electron Microscopy. Reviews by E. Rutter and H. Stünitz are gratefully acknowledged.

References

Beach, A., 1980. Retrogressive metamorphic processes in shear zones with special reference to the Lewisian complex. Journal of Structural Geology 2, 257–264.
Bloomfield, J.P., Covey-Crump, S.J., 1993. Correlating mechanical data with microstructural observations. Journal of Structural Geology 15, 1007–1019.
Boullier, A.M., Gueguen, Y., 1975. SP-mylonites: origin of some mylonites by superplastic flow. Contributions to Mineralogy and Petrology 50, 93–104.
de Bresser, J.H.P., ter Heege, J.H., Spiers, C.J., 2001. Grain size reduction by dynamic recrystallization: can it result in major theological weakening? International Journal of Earth Science 90 (1), 28–45.
de Bresser, J.H.P., Peach, C.J., Reijs, J.P.J., Spiers, C.J., 1998. On dynamic recrystallization during solid state flow: effects of stress and temperature. Geophysical Research Letters 25 (18), 3457–3460.
ten Brink, C.E., 1996. Development of porphyroclast geometries during non-co-axial flow. An experimental and analytical investigation. Geologica Ultraiectina 142, 163.
Brodie, K.H., 1980. Variations in mineral chemistry across a phlogopite peridotite shear zone. Journal of Structural Geology 2, 265–272.
Brodie, K.H., Rutter, E.H., 1987. The role of transiently fine-grained reaction products in syntectonic metamorphism: natural and experimental examples. Canadian Journal of Earth Science 24, 556–564.
Dell'Angelo, L.N., Tullis, J., 1996. Textural and mechanical evolution with progressive strain in experimentally deformed aplite. Tectonophysics 256, 57–82.
Denghui, J., Karato, S.-I., Obata, M., 1998. Mechanisms of shear localization in the continental lithosphere: inference from the deformation microstructures of peridotites from the Ivrea zone, northwestern Italy. Journal of Structural Geology 20 (2–3), 195–209.
Dijkstra, A.H., Drury, M.R., Vissers, R.L.M., Newman, J., 2002. Peridotite tectonites and mylonites in the Othris massif (Greece). Melt-rock Reaction and Shear Zone Formation Journal of Structural Geology 24, 1431–1450.
Drury, M.R., Vissers, R.L.M., van der Wal, D., HoogerduijnStrating, E.H., 1991. Shear localisation in upper mantle peridotites. Pure and Applied Geophysics 137 (4), 439–460.
Drury, M.R., Humphreys, F.J., 1988. The development of microstructure in Al–5% Mg during high temperature deformation. Acta Metallurgica 34, 2259–2271.
ECORS, 1988. The ECORS deep reflection seismic survey across the Pyrenees. Nature 331, 508–510.
Fabriès, J., Lorand, J.P., Bodinier, J.L., Dupuy, C., 1991. Evolution of the upper mantle beneath the Pyrenees: evidence from orogenic spinel lherzolite massifs. Journal of Petrology, Special Lherzolite Issue, 55–76.
Fitz Gerald, J.D., Stünitz, H., 1993. Deformation of granitoids at low metamorphic grade. I: reactions and grain size reduction. Tectonophysics 221, 269–297.
Fliervoet, T.F., Drury, M.R., Chopra, P.N., 1999. Crystallographic preferred orientations and misorientations in some olivine rocks deformed by diffusion or dislocation creep. Tectonophysics 303, 1–27.

Furusho, M., Kanagawa, K., 1999. Transformation-induced strain localization in a lherzolite mylonite from the Hidaka metamorphic belt of central Hokkaido, Japan. Tectonophysics 313, 411–432.
Govers, R., Wortel, M.J.R., 1995. Extension of stable continental lithosphere and the initiation of lithosphere scale faults. Tectonics 14 (4), 1041–1055.
Handy, M.R., 1989. Deformation regimes and the rheological evolution of fault zones in the lithosphere: the effects of pressure, temperature, grainsize and time. Tectonophysics 163, 119–152.
Handy, M., 1990. The solid-state flow of polymineralic rocks. Journal of Geophysical Research 96 (B6), 8647–8661.
Handy, M.R., 1994. Flow laws for rocks containing two non-linear viscous phases: a phenomenological approach (the corrected form). Journal of Structural Geology 16, 287–301.
Handy M.R., Stünitz, H, 2002. Strain localization by fracturing and reaction weakening – a mechanism for initiating exhumation of subcontinental mantle beneath rifted margins. In: Meer, S., Drury, M.R., de Bresser, J.H.P. and Pennock, GM. (Eds.), Deformation Mechanisms, Rheology and Tectonics: Current Status and Future Perspectives, Special Publication of the Geological Society.
Heilbronner, R., Tullis, J., 2002. The effect of strain annealing on microstructure and crystallographic preferred orientations of quartzites experimentally deformed in axial compression and shear. In: Geological Society [London] Special Publication, vol. 200 191–218.
Holyoke III, C.W., Tullis, J., 2006. Mechanisms of weak phase interconnection and the effects of phase strength contrast on fabric development. Journal of Structural Geology 28, 621–640.
Jaroslow, G.E., Hirth, G., Dick, H.J.B., 1996. Abyssal peridotite mylonites: implications for grain-size sensitive flow and strainlocalization in the oceanic lithosphere. Tectonophysics 256, 17–37.
Jessell, M.W., Bons, P.D., Griera, A., Evans, L.A., Wilson, J.L., 2009. A tale of two viscosities. Journal of Structural Geology 31, 719–736.
Jin, D.H., Karato, S., Obata, M., 1998. Mechanisms of shear localization in the continental lithosphere: inference from the deformation microstructures of peridotites from the Ivrea zone, northwestern Italy. Journal of Structural Geology 20 (2–3), 195–209.
Jordan, P.G., 1987. The deformational behavior of bimineralic limestone-halite aggregates. Tectonophysics 135, 185–197.
Kohlstedt, D.L., Goetze, C., Durham, W.B., VanderSande, J.B., 1976. New technique for decorating dislocations in olivine. Science 191, 1045–1046.
Kruse, R., Stünitz, H., 1999. Deformation mechanisms and phase distribution in mafic high-temperature mylonites from the Jotun Nappe, southern Norway. Tectonophysics 303, 223–249.
Michibayashi, K., Mainprice, D., 2004. The role of pre-existing mechanical anisotropy on shear zone development within oceanic mantle lithosphere: an example from the Oman ophiolite. Journal of Petrology 45, 405–414.
Mitra, G., 1978. Ductile deformation zones and mylonites: the mechanical processes involved in the deformation of crystalline basement rocks. American Journal of Science 278, 1057–1084.
Mitra, G., 1984. Brittle to ductile transition due to large strains along the white rock thrust, wind river mountains, Wyoming. Journal of Structural Geology 6 (1/2), 51–61.
Montési, L.G.J., Zuber, M.T., 2002. Parametric analysis of localization during a variety of geological conditions. Journal of Geophysical Research 107, B3. doi:10.1029/2001JB000465.
Neumann, B., 2000. Texture development of recrystallised quartz polycrystals unravelled by orientation and misorientation characteristics. Journal of Structural Geology 22 (11–12), 1695–1711.
Newman, J., Lamb, W.M., Drury, M.R., L, M., V, R., 1999. Deformation processes in a peridotite shear zone: reaction-softening by an H_2O-deficient, continuous net transfer reaction. Tectonophysics 303, 193–222.
Newman, J., Mitra, G., 1993. Lateral variations in mylonite zone thickness as influenced by fluid-rock interactions, Linville Falls fault, North Carolina. Journal of Structural Geology 15, 849–863.
Nicolas, A., 1986. Structure and petrology of peridotites: clues to their geodynamic environment. Reviews in Geophysics 24, 875–895.
Nicolas, A., Poirier, J.P., 1976. Crystalline Plasticity and Solid State Flow in Metamorphic Rocks. Wiley, New York.
O'Hara, K., 1988. Fluid flow and volume loss during mylonitization: an origin for phyllonite in an overthrust setting, North Carolina, U.S.A. Tectonophysics 156, 21–36.
O'Hara, K., 1990. State of strain in mylonites from the western blue ridge province, southern Appalachians: the role of volume loss. Journal of Structural Geology 12, 419–430.
Passchier, C.W., Trouw, R.A.J., 2005. Microtectonics. Springer, Berlin.
Prior, D.J., Boyle, A.P., Brenker, F., Cheadle, M.C., Day, A., Lopez, G., Peruzzo, L., Potts, G.J., Reddy, S., Spiess, R., Timms, N.E., Trimby, P., Wheeler, J., Zetterstrom, L., 1999. The application of electron backscatter diffraction and orientation contrast imaging in the SEM to textural problems in rocks. American Mineralogist 84 (11–12), 1741–1759.
Rubie, D.C., 1983. Reaction enhanced ductility; the role of solid-solid univariant reactions in the deformation of the crust and mantle. Tectonophysics 96, 331–352.
Rutter, E.H., Brodie, K., 1988. The role of tectonic grain size reduction in the rheological stratification of the lithosphere. Geologische Rundschau 77 (1), 295–308.
Rybacki, E., Dresen, G., 2004. Deformation mechanism maps for feldspar rocks. Tectonophysics 382, 173–187.
Sakai, T., Jonas, J.J., 1984. Overview No-35-dynamic recrystallization – mechanical and microstructural considerations. Acta Metallurgica 32 (2), 189–209.
Schmid, S., Boland, J.N., Paterson, M.S., 1977. Superplastic flow in finegrained limestone. Tectonophyics 43, 257–291.
Spry, A., 1983. Metamorphic Textures. Pergamon Press, Oxford, England.
Stünitz, H., 1998. Syndeformational recrystallization – dynamic or compositionally induced? Contributions to Mineralogy and Petrology 131, 219–236.
Stünitz, H., Fitz Gerald, J.D., 1993. Deformation of granitoids at low metamorphic grade. II: granular flow in albite-rich mylonites. Tectonophyiscs 221, 299–324.
Sundberg, M., Cooper, R.F., 2008. Crystallographic preferred orientation produced by diffusional creep of harzburgite: effects of chemical interactions among phases during plastic flow. Journal of Geophysical Research 113, B12208.
Takeda, Y.-.T., Griera, A., 2006. Rheological and kinematical responses to flow of two-phase rocks. Tectonophysics 427, 95–114.
Tharp, T.M., 1983. Analogies between the high temperature deformation of polyphase rocks and the mechanical behavior of porous powder metal. Tectonophysics 96, T1–T11.
Toy, V., Newman, J., Lamb, W., Tikoff, B., 2010. The role of pyroxenites in formation of shear instabilities in the mantle: evidence from an ultramafic ultramylonite, Twin Sisters Massif, Washington. Journal of Petrology 51 (1–2), 55–80.
Trimby, P.W., Drury, M.R., Spiers, C.J., 2000. Recognising the crystallographic signature of recrystallisation processes in deformed rocks: a study of experimentally deformed rocksalt. Journal of Structural Geology 22 (11–12), 1609–1620.
Trimby, P.W., Prior, D.J., Wheeler, J., 1998. Grain boundary hierarchy development in a quartz mylonite. Journal of Structural Geology 20, 917–935.
Van den Driessche, J., Brun, J.-P., 1987. Rolling structures at large shear strain. Journal of Structural Geology 9, 691–704.
Vissers, R.L.M., Drury, M.R., Hoogerduijn Strating, E.H., Spiers, C.J., van der Wal, D., 1995. Mantle shear zones and their effect on lithosphere strength during continental breakup. Tectonophysics 249, 155–171.
Vissers, R.L.M., Drury, M.R., Hoogerduijn Strating, E.H., van der Wal, D., 1991. Shear zones in the upper mantle: a case study in an alpine lherzolite massif. Geology 19, 990–993.
Vissers, R.L.M., Drury, M.R., Newman, J., Fliervoet, T.F., 1997. Mylonitic deformation in upper mantle peridotites of the North Pyrenean Zone (S France): implications for strength and strain localization in the lithosphere. Tectonophysics 279, 303–325.
Wang, Z.C., Dresen, G., Wirth, R., 1996. Diffusion creep of fine-grained polycrystalline anorthite at high temperature. Geophysical Research Letters 23, 3111–3114.
Wang, Z.C., Ji, S.C., 2000. Diffusion creep of fine-grained garnetite: implications for the flow strength of subducting slabs. Geophysical Research Letters 27 (15), 2333–2336.
Warren, J.M., Hirth, G., 2006. Grain size sensitive deformation mechanisms in naturally deformed peridotites. Earth and Planetary Science Letters 248, 438–450.
Warren, J.M., Hirth, G., Kelemen, P.B., 2008. Evolution of olivine lattice preferred orientation during simple shear in the mantle. Earth and Planetary Science Letters 272, 501–512.
Webber, C.W., Little, T., Newman, J., Tikoff, B., 2008. Fabric superposition in upper mantle peridotite, Red Hills, New Zealand. Journal of Structural Geology 30, 1412–1428.
Webber, C., Newman, J., Holyoke, C.W.III, Little, T., Tikoff, B., 2010. Fabric Development in Cm-scale Shear Zones in Ultramafic Rocks, Red Hills, New Zealand.
White, S.H., Burrows, S.E., Carreras, J., Shaw, N.D., Humphreys, F.J., 1980. On mylonites in ductile shear zones. Journal of Structural Geology 2 (1/2), 175–187.
Wintsch, R.P., Dunning, J., 1985. The effect of dislocation density on the aqueous solubility of quartz and some geologic implications – a theoretical approach. Journal of Geophysical Research-Solid Earth and Planets 90, 3649–3657.